Proposal for a Pulse-Compression Scheme in X-Ray Free-Electron Lasers to Generate a Multiterawatt, Attosecond X-Ray Pulse

Takashi Tanaka*

RIKEN SPring-8 Center, Koto 1-1-1, Sayo, Hyogo 679-5148, Japan

(Received 6 November 2012; published 20 February 2013)

A novel scheme to compress the radiation pulse in x-ray free electron lasers is proposed not only to shorten the pulse length but also to enhance the peak power of the radiation, by inducing a periodic current enhancement with an optical laser and applying a temporal shift between the optical and electron beams. Calculations show that a 10-keV x-ray pulse with a peak power of 5 TW and a pulse length of 50 asec can be generated by applying this scheme to an existing x-ray free electron laser facility.

DOI: 10.1103/PhysRevLett.110.084801 PACS numbers: 41.60.Cr, 42.55.Vc

The advent of x-ray free electron lasers (XFELs) based on a self-amplified spontaneous emission (SASE) scheme, such as the Linac Coherent Light Source [1] and the SPring-8 Angstrom Compact free electron LAser (SACLA) [2], has extended the wavelength availability of laser sources to angstrom wavelength regions. Although the SASE-based XFEL produces spatially coherent and extremely powerful photon beams as in the optical lasers, there has been one deficiency that the startup from shot noise leads to poor temporal coherence. Recently, a self-seeding technique was demonstrated in the Linac Coherent Light Source [3], which significantly improves the temporal coherence and thus leads to an enhancement of photon flux and brilliance. Nevertheless, there still remains one important technical challenge in XFELs: a pulse compression technique that enables us to enhance the peak power as well as shorten the pulse length, which is commonly applied to optical lasers to produce a femtosecond-terawatt light pulse [4–6].

Up to now, many ideas have been proposed to shorten the XFEL pulse length [7–21]; however, none of them lead to an enhancement of the peak power because only a small portion of electrons contribute to lasing in these schemes. In this Letter, we propose a new scheme to compress the XFEL pulse not only to shorten the pulse length down to several tens of attoseconds but also to enhance the peak power up to several terawatts.

Figure 1 shows the schematic illustration of the accelerator layout to realize the proposed XFEL pulse compression scheme. In addition to ordinary accelerator components, two extra elements are added, which are originally proposed to shorten the XFEL pulse length. One is the slotted foil [8] inserted in the bunch compressor (BC) section where the longitudinal coordinate s in the electron bunch is strongly correlated with the horizontal coordinate x. The foil spoils the electron beam emittance in the head and tail parts of the bunch and suppresses lasing there. Note that the slot is set relatively wide in our scheme because its function is not to shorten the pulse length as in the original proposal but to set a defined temporal window of lasing and define the lasing domain in the electron bunch. The other is the section to apply the enhanced SASE (ESASE) scheme [14], in which an optical laser (ESASE laser) having a wavelength of λ_E is injected synchronously with the electron bunch to a wiggler whose fundamental wavelength equals λ_E. This induces a regularly spaced energy modulation, which is converted to a density modulation in the dispersive chicane that follows the wiggler. Note that coherent emission from such an electron beam with the laser-induced modulation has been theoretically investigated in Refs. [22,23].

The current distribution after the above two processes is roughly given by

$$I(s) = [I_o(s) + I_u(s)]E(s),$$

where $I_o(s)$ and $I_u(s)$ denote the current distributions just after the BC section. The former corresponds to the electrons that contribute to lasing without being scattered by the foil, while the latter corresponds to the scattered electrons, which do not contribute to lasing. The effect of the slotted foil is reduced by the intrinsic horizontal beam size at the position of the foil insertion, which is determined by the emittance, betatron function, and uncorrelated energy spread. Approximating these impacts on the current distribution by the Gaussian function with the standard deviation of σ_f, we have

$$I_o(s) = \frac{1}{\sqrt{2\pi}\sigma_f}\int_{s_1}^{s_2} I(s')\exp\left[-\frac{(s-s')^2}{2\sigma_f^2}\right]ds',$$

$$I_u(s) = I(s) - I_o(s),$$

where the longitudinal positions s_1 and s_2 are correlated with the horizontal positions defining the slot width of the foil, and $I(s)$ denotes the current distribution in the case that no foil is inserted.

$E(s)$ is a periodic function with a period of λ_E and denotes the current enhancement by the ESASE scheme. Under the condition when the momentum compaction in the dispersive chicane is optimized, $E(s)$ is given by [14]

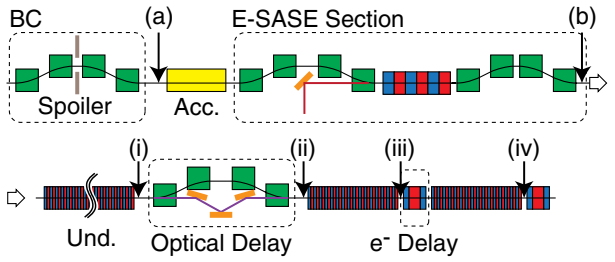

FIG. 1 (color online). Accelerator layout to realize the proposed pulse compression scheme.

$$E(s) = \sum_j \frac{eB}{1+B^{1/e}} \frac{1}{1+16B^2[(s/\lambda_E)-(\theta/2\pi)-j]^2},$$

with $B = \Delta\gamma/\sigma_\gamma$, where $\Delta\gamma$ is the amplitude of the energy modulation induced by the ESASE laser, σ_γ is the rms uncorrelated energy spread of the electron bunch, and e is the base of the natural logarithm. The phase parameter θ denotes the timing jitter between the electron bunch and the ESASE laser and fluctuates randomly between $-\pi$ and π from shot to shot.

Using the above equations, the current distributions after the respective sections have been calculated for an electron bunch having a Gaussian temporal profile with a peak current of 3.5 kA and a FWHM bunch length of 40 fsec. Figure 2(a) shows the current distribution just after the BC section, where $s_1 = -4.4\,\mu$m, $s_2 = 3.6\ \mu$m, and $\sigma_f = 0.2\ \mu$m have been assumed. Compared to the original Gaussian function, the temporal window of lasing is found

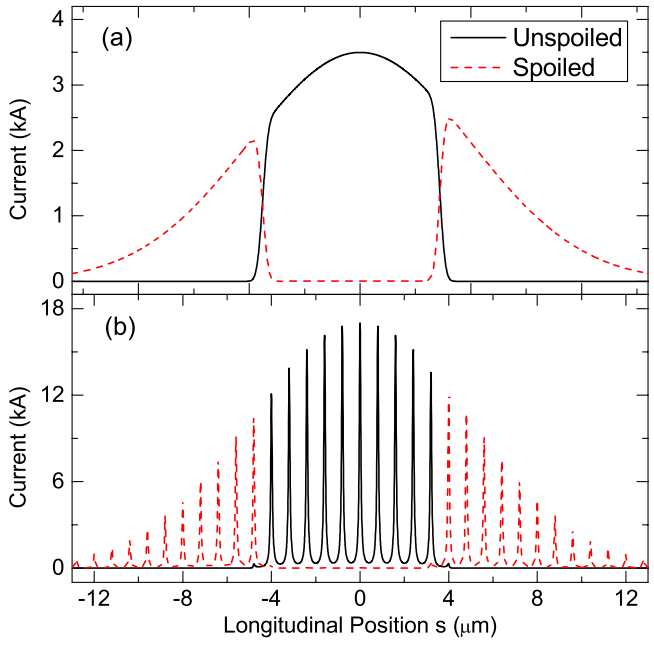

FIG. 2 (color online). Calculated current distributions after (a) the bunch compressor with the slotted foil and (b) ESASE sections.

to be definitely confined; however, the boundary is not sharply truncated and a fringe region exists, whose width corresponds to σ_f. In Fig. 2(b), the current distribution after the ESASE section is shown, where $\lambda_E = 800$ nm, $B = 5$, and $\theta = 0$ have been assumed. A comblike current distribution having a pitch of 800 nm is generated with the peak current being enhanced approximately by a factor of 5. The ESASE laser power to obtain the energy modulation of $\Delta\gamma/\sigma_\gamma = 5$ is estimated to be nearly 1 GW when an 8-GeV electron bunch with an uncorrelated energy spread of $\sigma_\gamma/\gamma = 10^{-4}$ is injected to a ten-period wiggler. This corresponds to a pulse energy of 1 mJ, which is feasible enough with the state-of-the-art laser technology, even if a relatively long pulse length of 1 psec is assumed. Such a long-pulse ESASE laser helps to relax the tolerance of temporal synchronization with the electron bunch.

Now let us explain the processes of how to generate and amplify a single x-ray pulse with an electron bunch having a comblike current distribution. The pulse growth after each amplification process is schematically illustrated in Fig. 3. Also refer to the numbers indicated in Fig. 1 for the positions in the undulator line corresponding to the respective processes.

First, a pulse train with an interval of λ_E is generated by the normal SASE process, which reflects the comblike structure of the current distribution (i). The undulator length in this process should be adjusted so that each x-ray pulse is not saturated and the electron quality is not degraded.

Next, the electron bunch is separated from radiation using a magnetic chicane. Instead of installing a monochromator in the self-seeding scheme, a set of reflective mirrors is installed to give a temporal delay to the radiation relative to the electron bunch [24], in order to shift the pulse train backward along the electron bunch (ii). The length of the backward shift should be equal to $(N_{pk}-1)\lambda_E$, where N_{pk} is the number of current peaks existing in the lasing domain. This is a condition to synchronize the leading x-ray pulse in the train (target pulse)

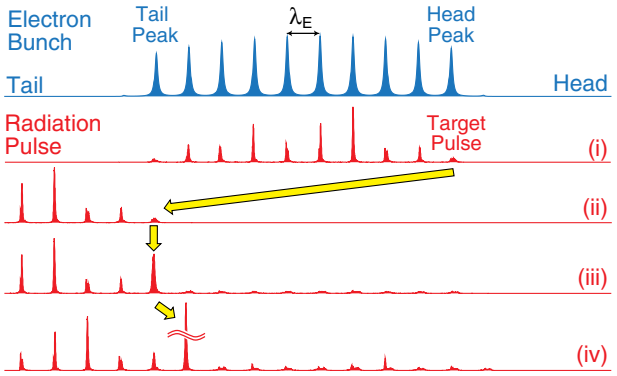

FIG. 3 (color online). X-ray pulse growth in the early stage of FEL amplification.

with the current peak located at the tail end of the lasing domain (tail peak).

Although the SASE-induced microbunch is washed out while the electron bunch passes through the chicane, an amplification process is immediately launched in the following undulator segment at the tail peak position because the target pulse works as a seeding light, while the rest of the x-ray pulses that slip out of the lasing domain are not amplified (iii). At other current peak positions, the normal SASE process is dominant because no seeding light is present. It is therefore possible to suppress the x-ray pulse generation at these current peaks by limiting the length of the undulator. To summarize, only the target pulse is selectively amplified in this process.

After the target pulse is sufficiently amplified by the tail peak, it is shifted forward by the distance of λ_E by giving a temporal delay to the electron bunch using a magnetic chicane. The target pulse is then positioned at the fresh current peak where the beam quality degradation (i.e., the increase of the energy spread) is not significant, and the amplification of the target pulse continues (iv). It should be noted that the x-ray pulse just behind the target pulse arrives at the tail peak, which might be amplified. Its amplification gain is, however, considerably low because the beam quality at the tail peak position is already degraded by the former interaction with the target pulse.

Repeating the above process (iv) until the target pulse arrives at the leading current peak in the lasing domain (head peak), the intensity of the target pulse is drastically enhanced. If there are still more undulator segments available, the amplification of the target pulse can be continued by shifting it backward to the position of the tail peak.

To illustrate a possible performance of the proposed scheme, free electron laser (FEL) simulations have been performed under the assumption that an 8-GeV electron bunch with a normalized emittance of 0.7 μm and an uncorrelated energy spread of 10^{-4} is injected to the undulators with a K value of 2.18 and magnetic period of 18 mm, which are currently available in SACLA [2]. Although up to 26 undulator segments with a length of 5 m can be installed in SACLA, the total segment number has been assumed to be 24 excluding two segments for installation of the optical-delay chicane that needs a relatively long space.

As an example, the current distribution shown in Fig. 2(b) is assumed. Note that the bunch charge of the electron beam in SACLA, which actually contributes to lasing, has been deduced to be 75 pC with a peak current of 3.5 kA and a FWHM bunch length of 20 fsec [2]. The bunch length of 40 fsec assumed in the simulation is thus double the present value. It should be emphasized, however, that an upgrade program to expand the bunch length is under progress in SACLA to increase the pulse energy of the radiation, and the 40-fsec bunch length will presumably

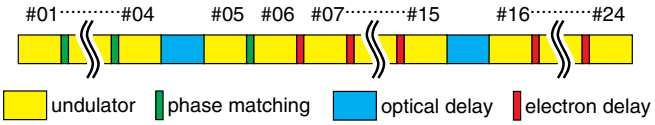

FIG. 4 (color online). Layout of the undulator, and optical- and electron-delay chicanes assumed in the calculation.

be available in the near future. With the above parameters, a 10-keV x-ray pulse with an averaged peak power of 20 GW and a pulse length of 20 fsec is expected near saturation through a conventional SASE process.

The undulator layout including the electron- and optical-delay chicanes has been optimized to maximize the peak power and improve the contrast of the target pulse against others and is shown in Fig. 4. Note that each undulator segment is assumed to be 5 m long as in SACLA. The initial four segments correspond to process (i) and the following optical delay corresponds to process (ii). The target pulse is amplified in two segments after the chicane, and then is shifted forward to the fresh current peak by the electron-delay chicane placed at the exit of each segment. After arriving at the head peak at the 15th segment, the target pulse is shifted backward to the tail peak again and the amplification continues. All the calculations and simulations have been carried out with SIMPLEX, a FEL simulation code developed at SPring-8 [25]. Note that the ESASE process not only enhances the peak current but also increases the energy spread at the current peak positions [14], which has been taken into account in the FEL simulations.

Figure 5 shows the calculated temporal structures of the radiation just after the 4th, 7th, 10th, and 24th (final) segments. Note that the K values and the optical and electron delays in respective segments have been slightly modified to maximize the peak power of the target pulse, the details of which are to be presented elsewhere.

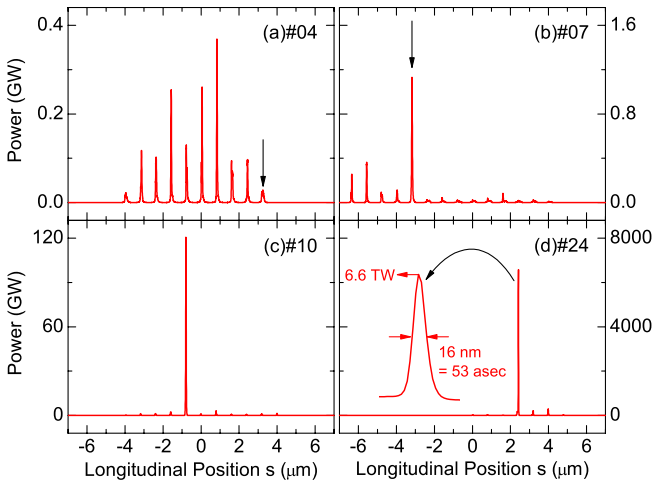

FIG. 5 (color online). X-ray pulse temporal structures calculated at the ends of different undulator segments.

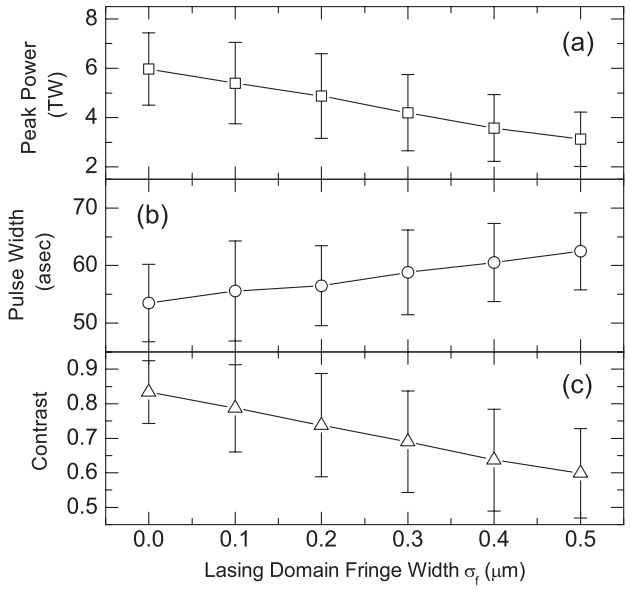

FIG. 6. Impacts of the fringe width on (a) the peak power, (b) pulse length and (c) contrast.

At the exit of the 4th segment [see Fig. 5(a)], several x-ray pulses are found at the current peak positions. Among them, the target pulse indicated by an arrow is selectively amplified in the following segments by applying appropriate optical and electron delays, which leads to formation of a solitary pulse at the exit of the 10th segment as shown in Fig. 5(c). The target pulse is exponentially amplified up to this segment and the peak power reaches nearly 100 GW, being comparable to the saturation power in the conventional SASE process estimated with the beam parameters at the center of the electron bunch having a peak current of 17 kA [refer to Fig. 2(b)]. It should be stressed that the target pulse is not saturated there, but is further amplified by being sequentially shifted to the fresh current peaks, although the amplification is not exponential but nearly quadratic in this region. This is similar to the superradiant FEL regime [26–28], in which the peak power of radiation grows quadratically with the undulator length. As a result, the target pulse finally evolves into an extremely intense x-ray pulse with a peak power of 6.6 TW and a FWHM pulse length of 53 asec [Fig. 5(d)]. Compared to the original values (20 GW and 20 fsec) without applying the proposed scheme, the SASE pulse has been compressed by a factor of 300.

In Fig. 5(d), we find that several satellite pulses, albeit weak ones in this example, exist in addition to the target pulse. The growth of these satellite pulses not only reduces the contrast but also the peak power of the target pulse by degrading the electron beam quality at the current peak positions before arrival of the target pulse. It is thus important to suppress the generation of x-ray pulses other than the target pulse in the early stage of FEL amplification, which is actually done in process (ii) by shifting the target pulse generated at the head peak backward to the tail peak. It should be noted, however, that the interval Δs between the two peak positions might fluctuate from shot to shot because of the stochastic nature of the SASE process and the timing jitter between the electron bunch and the ESASE laser.

The stability of Δs depends on σ_f/λ_E, i.e., the ratio of the fringe width of the lasing domain to the wavelength of the ESASE laser. When σ_f is much shorter than λ_E, N_{pk} is clearly defined as in the current distribution shown in Fig. 2(b) and thus Δs is expected to be nearly constant in every shot. This is not the case when σ_f is comparable to or larger than λ_E, in which case N_{pk} cannot be clearly defined and thus Δs is supposed to fluctuate discretely with a discrete interval of λ_E.

In order to evaluate the impact of the fringe width σ_f on the performance of the proposed scheme, FEL simulations have been repeated with the same parameters and conditions as those used in Fig. 5, except for three parameters: σ_f, θ, and i, where i is the initial seed for the random number generator to simulate the shot noise. In order to consider the shot-to-shot fluctuation, 240 sets of simulations have been performed, with σ_f being fixed at a certain number, θ being uniformly swept in the range $(-\pi, +\pi)$, and i being continuously varied to change the shot-noise condition. From each simulation result, the peak power, pulse length, and contrast defined by the percentage of the photon intensity contained in the target pulse have been retrieved, and their average and standard deviations have been calculated as functions of σ_f. The calculation results are plotted in Fig. 6, where we find that the peak power and contrast decrease and the pulse length increases with an increase in the value of σ_f. It is thus concluded that the effectiveness of the proposed scheme strongly depends on how short the parameter σ_f can be, which is related to the accelerator design of the facility and is outside the scope of this Letter. Useful information is found in Ref. [9], where a detailed discussion is given concerning the production of an extremely short SASE pulse by means of the slotted foil scheme. It is reported that an electron bunch having a lasing domain length of 1.3 fsec in FWHM is available by a careful choice of accelerator parameters. This can be roughly converted to a value for σ_f of 0.166 μm, which is short enough for this new scheme to work effectively.

*ztanaka@spring8.or.jp

[1] P. Emma *et al.*, Nat. Photonics **4**, 641 (2010).
[2] T. Ishikawa *et al.*, Nat. Photonics **6**, 540 (2012).
[3] J. Amann *et al.*, Nat. Photonics **6**, 693 (2012).
[4] C. V. Shank, R. L. Fork, R. Yen, R. H. Stolen, and W. J. Tomlinson, Appl. Phys. Lett. **40**, 761 (1982).
[5] M. Nisoli, S. De Silvestri, and O. Svelto, Appl. Phys. Lett. **68**, 2793 (1996).

[6] A. Suda, M. Hatayama, K. Nagasaka, and K. Midorikawa, Appl. Phys. Lett. **86**, 111116 (2005).
[7] E. L. Saldin, E. A. Schneidmiller, and M. V. Yurkov, Opt. Commun. **212**, 377 (2002).
[8] P. Emma, K. Bane, M. Cornacchia, Z. Huang, H. Schlarb, G. Stupakov, and D. Walz, Phys. Rev. Lett. **92**, 074801 (2004).
[9] P. Emma, Z. Huang, and M. Borland, in *Proceedings of FEL 2004* (JACoW, Trieste, Italy, 2004), p. 333.
[10] S. Reiche, P. Musumeci, C. Pellegrini, and J. B. Rosenzweig, Nucl. Instrum. Methods Phys. Res., Sect. A **593**, 45 (2008).
[11] Y. Ding *et al.*, Phys. Rev. Lett. **102**, 254801 (2009).
[12] E. L. Saldin, E. A. Schneidmiller, and M. V. Yurkov, Opt. Commun. **239**, 161 (2004).
[13] A. A. Zholents and W. M. Fawley, Phys. Rev. Lett. **92**, 224801 (2004).
[14] A. A. Zholents, Phys. Rev. ST Accel. Beams **8**, 040701 (2005).
[15] A. A. Zholents and G. Penn, Phys. Rev. ST Accel. Beams **8**, 050704 (2005).
[16] E. L. Saldin, E. A. Schneidmiller, and M. V. Yurkov, Phys. Rev. ST Accel. Beams **9**, 050702 (2006).
[17] W. M. Fawley, Nucl. Instrum. Methods Phys. Res., Sect. A **593**, 111 (2008).
[18] A. A. Zholents and M. S. Zolotorev, New J. Phys. **10**, 025005 (2008).
[19] D. Xiang, Z. Huang, and G. Stupakov, Phys. Rev. ST Accel. Beams **12**, 060701 (2009).
[20] Y. Ding, Z. Huang, D. Ratner, P. Bucksbaum, and H. Merdji, Phys. Rev. ST Accel. Beams **12**, 060703 (2009).
[21] N. R. Thompson and B. W. J. McNeil, Phys. Rev. Lett. **100**, 203901 (2008).
[22] H. K. Avetissian and G. F. Mkrtchian, Nucl. Instrum. Methods Phys. Res., Sect. A **483**, 548 (2002).
[23] H. K. Avetissian, *Relativistic Nonlinear Electrodynamics* (Springer, New York, 2006), Chap. 8.
[24] G. Geloni, V. Kocharyan, and E. Saldin, DESY Report No. 10-004.
[25] T. Tanaka, in *Proceedings of FEL 2004* (JACoW, Trieste, Italy, 2004), p. 435.
[26] R. Bonifacio, L. De Salvo, P. Pierini, and N. Piovella, Nucl. Instrum. Methods Phys. Res., Sect. A **296**, 358 (1990).
[27] R. Bonifacio, N. Piovella, and B. W. J. McNeil, Phys. Rev. A **44**, R3441 (1991).
[28] L. Giannessi, P. Musumeci, and S. Spampinati, J. Appl. Phys. **98**, 043110 (2005).